18

ATMOSPHERIC MODELS

F. KENTON MUSGRAVE, LARRY GRITZ,
AND STEVEN WORLEY

INTRODUCTION

Even more than the last chapter, this chapter is highly technical and may be of interest only to mathematically minded programmers. You might just want to read this introduction, which is written at a fairly conversational level. The rest of this chapter was originally written as a technical paper, so most of the prose is pretty dry and terse.

Rendering realistic atmospheric effects involves three distinct elements: scattering models, geometric atmospheric density distribution (GADD) models, and numerical integration schemes for each. We present a series of simple, continuous GADD models of increasing geometric fidelity to spherical planetary atmospheres and integration schemes for each. We describe a RenderMan implementation of a planetary atmosphere and a general GADD integration scheme with bounded numerical error. We also suggest a simplified approximation of Rayleigh scattering. These models are distinctly nonphysical, ontogenetic models designed to be useful for production image synthesis rather than to provide accurate simulations. The GADDs we present and their associated integration schemes can, however, be coupled to published physical scattering models to augment the accuracy of those models.

Landscape painters have known for hundreds of years that *aerial perspective,* the bluing and loss of contrast with distance, is the primary visual cue indicating large physical scale in a rendering (Gedzelman 1991).[1] These effects are due to

1. Shannon (1995) points out that artists break aerial perspective into two components: *atmospheric perspective* and *color perspective.* The former is the change in contrast with distance, due to noncolored haze. The latter is the change in color with distance, light backdrops becoming redder and dark ones bluer, due to Rayleigh scattering. For more on this topic see *www.kenmusgrave.com/4_persp.html.*

atmospheric scattering of light. In the scientific literature these effects are described by the Rayleigh and Mie scattering models. Previous authors (Klassen 1987; Nishita et al. 1993; Tadamura et al. 1993) have presented physical models of Rayleigh and Mie scattering. Efficiency of light scattering is modulated in part by the density of the atmosphere, which in turn varies spatially. This variation is not only with altitude: altitude is a function of the radius from the center of a planet, thus at the largest scales, the atmosphere must curve around a planet. We call a model describing the spatial distribution of atmospheric density *geometric atmospheric density distribution* (GADD). In Klassen (1987) the GADD consists of two horizontal slabs of constant density; Nishita et al. (1993) uses concentric shells of linearly interpolated density. We present some continuous GADDs to improve upon those models.

The global context for a landscape is the surface of a planet. In that context, all optical paths, defined as a ray's extent in a participating medium, are finite since they either intersect a surface, are absorbed or scattered, or exit the atmosphere due to its curvature around the planet. The spatial distribution of a GADD can affect its accuracy as a function of scale: the simplest, homogeneous GADD is accurate for small scales, an intermediate-scale model may take into account change in density with height, while a global GADD should take into account both change in density with altitude and the curvature of the atmosphere. (Modeling the true complexity of atmospheric structure remains impractical.) We will describe both local and global GADD models, along with methods for integrating their optical density along arbitrary ray paths. The local GADD models may be integrated analytically. We will describe numerical integration schemes for the global GADD functions. We also suggest a simple, computationally minimal approximation of Rayleigh scattering. Although nonphysical, this model produces an artistically sufficient model of aerial perspective without the unnecessary complications of physical models.

Although the models presented here are not physical models, they may in some cases represent improvements over published "physical" models. We claim that they are visually effective and that they are recommended by Occam's Razor due to their simplicity. Most are not particularly novel, as they appear to have been repeatedly reinvented by different graphics researchers. Nevertheless, they have yet to be described in the mainstream graphics literature.

Blinn (1982a) pointed out that atmospherics involve two distinct types of models: scattering models and density distribution models. We assert that integration schemes for these models constitute a third essential element. Our goal is to address all three elements, to visual satisfaction, in as little computation as possible.

For our discussion, we define the *optical path* as the extent of a ray's passage through an atmosphere, *scattering* as redirection of direct illumination from a light source (implying single scattering) into the optical path and toward the view point, *outscattering* as redirection of light out of an optical path toward the view point, and *extinction* as the cumulative effect of both outscattering and absorption along the path.

BEER'S LAW AND HOMOGENEOUS FOG

As a light ray traverses an optical path, some light is extinguished and some light may be added by emission and/or scattering. As described in Max (1986), the sum of these effects can describe, physically, the behavior of a participating medium. (We discuss only atmospheres here, not general participating media such as glass, water, smoke, flames, clouds, and so forth.)

The effect of an atmosphere on the intensity of a light ray can be described by the differential equation

$$dI = \sigma(\vec{x}) + E(\vec{x})\,d\vec{x}$$

where x is the position in three dimensions, $\sigma(\vec{x})$ describes extinction per unit length, and $E(\vec{x})$ describes emission and scattering per unit length into the optical path. When σ and E are proportional to one another and are functions solely of position x, we can define *optical depth* τ as

$$\tau = \int_0^{t_e} \sigma(\vec{x})\,dt$$

the integral over the optical path of the GADD $\sigma(\vec{x})$. As in Haines (1989) we index the position along the ray by t, which ranges from 0 to t_e. Beer's law gives a physical solution to this simple model and gives us the transparency T over the optical path as a function of τ:

$$T = e^{-\tau}$$

For a homogeneous and isotropic GADD (i.e., $\sigma = c$, a constant), we have $\tau = ct_e$. Such homogeneous fog is fairly common in renderers; its effectiveness is due to its embodiment of a simple but physically accurate scattering model.

For simplicity, we consider extinction over the optical path to be $1 - T$. This extinguished portion of the intensity is replaced with the atmosphere color as a direct

consequence of the $E(\vec{x})$ term in the previous differential equation. In the models we present below, we ignore emission[2] but engineer the absorption rate σ to vary spatially. After obtaining τ by integrating σ, we may use Beer's law to accurately compute the true effect of the atmosphere, given a scattering model. We therefore concentrate most of the rest of our presentation on nonhomogeneous density models and their integration.

EXPONENTIAL MIST

A useful GADD for landscape renderings has a density distribution that varies as e^{-z}, where z is altitude relative to a horizontal plane. It features local fidelity to nature, as atmospheric optical density is known to vary exponentially with altitude (Lynch 1991). Behavior of this GADD can be parameterized as

$$\sigma = Ae^{-Bz}$$

where A controls the overall density and B controls the falloff of the density with altitude. Its effectiveness in a landscape rendering is illustrated in Figure 18.2. This GADD may be integrated analytically:

$$\tau = t_e \int_{z_o}^{z_e} e^{-z} dz = \frac{At_e}{Bz_d}\left(e^{-(z_o + z_d t_e)} - e^{-z_o}\right)$$

where z_0 is the z coordinate of the ray origin and z_d is the z component of the ray's normalized direction vector. For very small z_d, corresponding to nearly horizontal rays, we substitute

$$\tau = At_e e^{-Bz_o}$$

2. Although we do not model emission, a similar effect is nonetheless obtained. These are nonphysical scattering models, in which conservation of energy is not maintained. Because the atmosphere color does not depend on illumination, except in our last model, energy may appear in the optical path without illumination (e.g., the white color of an atmosphere that is actually in shadow). This nonphysicality can be used to artistic advantage, as illustrated in Figure 18.1, a rendering without any light sources. The color variation in that atmosphere is attained basically by reversing the order of the RGB values for the extinction coefficients on our simplified Rayleigh scattering model, from those used to get blue sky.

FIGURE 18.1 *Fractal Mandala* illustrates an alternative use of the planetary atmosphere and minimal Rayleigh scattering model. The color is obtained by changing values in the extinction coefficient vector from those used for Rayleigh scattering. Copyright © F. Kenton Musgrave.

FIGURE 18.2 *Carolina* illustrates both the exponential atmosphere and color perspective. Copyright © F. Kenton Musgrave.

the asymptotic value as z_d goes to zero, to prevent division by zero. This GADD has unbounded optical paths for horizontal rays. The optical path of such rays is ultimately limited by the finite numerical representation of infinity in the renderer; this value can be varied to limit integration.

A RADIALLY SYMMETRIC PLANETARY ATMOSPHERE

Because of the infinite optical paths cited earlier, a GADD that varies exponentially with radius from a central point is more realistic on large scales. For such a GADD, the radius r from the central point is related to position t along the ray as

$$r(t) = \sqrt{\alpha^2 + 2\beta t + t^2}$$

where α and β are constants determined by the ray path and the origin, or center, of the radial fog. This function forms a hyperbola. With σ given as this function of r, instead of computing

$$\int \sigma(t)\,dt$$

we must compute

$$\int \sigma\left(\sqrt{\alpha^2 + 2\beta t + t^2}\right)dt$$

which can prove challenging.

A simple radial GADD is

$$\sigma(r) = e^{-r^2}$$

This function cannot be integrated in closed form, but a numerical approximation is available in the C and FORTRAN math libraries in the *error function:*

$$erf(x) \approx \frac{2}{\pi}\int_0^x e^{-t^2}$$

This GADD may be parameterized as

$$\sigma = Ae^{-Br^2}$$

where A controls the overall density and B modulates falloff with radius. This GADD can provide convincing visual results (see Figure 20.4).

Consider integrating this GADD. For a ray origin $\vec{r}_0$ and unit direction $\vec{x}$, and a GADD origin $\vec{o}$, we have

$$r(t) = \sqrt{\alpha^2 + 2\beta t + t^2}$$

where $\alpha = |\vec{r}_O - \vec{o}|$ and $\beta = r_d \bullet (\vec{r}_O - \vec{o})$. We must compute

$$\tau = \int_0^{t_e} Ae^{-B(a^2+2\beta r+t^2)}dt$$

A solution to this integral is given by

$$\tau \approx \frac{A\sqrt{\pi}e^{-B(\alpha^2-\beta^2)}}{2\sqrt{B}}\left(erf\left(\sqrt{B}\,(t_e+\beta)\right) - erf\left(\beta\sqrt{B}\right)\right)$$

Unfortunately, the more physically plausible GADD $\sigma = e^{-r}$ cannot be reduced to such an expression, due to the complex dependence of r on t. Thus we may require a numerical integration method, ideally one that is tailored specifically to the

hyperbolic-quadratic exponential form of the equation and specific accuracy needed for rendering. We discuss this in a later section; for now we digress to scattering.

A MINIMAL RAYLEIGH SCATTERING APPROXIMATION

We require at least a first approximation of Rayleigh scattering to obtain proper coloration of the atmosphere. Single Rayleigh scattering adds blue light along an illuminated optical path; this is why the sky is blue. Rayleigh outscattering along the optical path reddens light coming from the background, causing, for instance, sunsets to be red. Similarly, direct light flux available for scattering is reddened; this effect is what often makes sunlight yellow. Although more elaborate and accurate models are available (Klassen 1987; Nishita et al. 1993), we have found the following extremely simple approximation to be sufficient for first-order visual realism. This model is responsible for all the atmospheric coloration effects seen in the figures from Chapters 14–19.

In our discussion so far, τ has been treated as a scalar value. In wavelength-dependent scattering, τ is a vector over wavelength λ, each λ sample having an independent value of τ. For Rayleigh scattering, τ is proportional to λ^{-4} (Klassen 1987). Each component of the τ vector requires a separate evaluation of the $e^{-\tau_\lambda}$ expression of Beer's law. Time complexity then varies linearly with the number of λ samples. The tristimulus nature of color vision dictates a minimum of three values for full-color images; hence the familiar triad of RGB samples. Larger numbers of samples, taken in the CIE XYZ color space, may yield more accurate colors (Hall 1989).

We simply note that expanding τ to an RGB vector can give a computationally minimal and visually pleasing approximation of Rayleigh scattering (see Figures 18.3 and 18.4). Correct discrete numerical integration of single scattering along the optical path requires raymarching with computation at each sample of the extinction of the direct illumination available for scattering. In the absence of such a correct but expensive scheme, extinction due to Rayleigh scattering along the optical path can be approximated by using a yellow-brown (smog-colored) atmosphere. In Figure 18.4 the RGB color of the atmosphere is `(1.0, 0.65, 0.5)` and τ = `(3.0, 7.5, 60.0)`. Observe that the atmosphere is blue against a black background, and a white background is filtered to orange, as illustrated in Figure 18.5. Figure 18.4 illustrates that the horizon still appears white against a black background, largely due to psychoperceptual reasons—it is actually no more white than the smoggy atmosphere color. We recommend this simplest model for maximally efficient rendering.

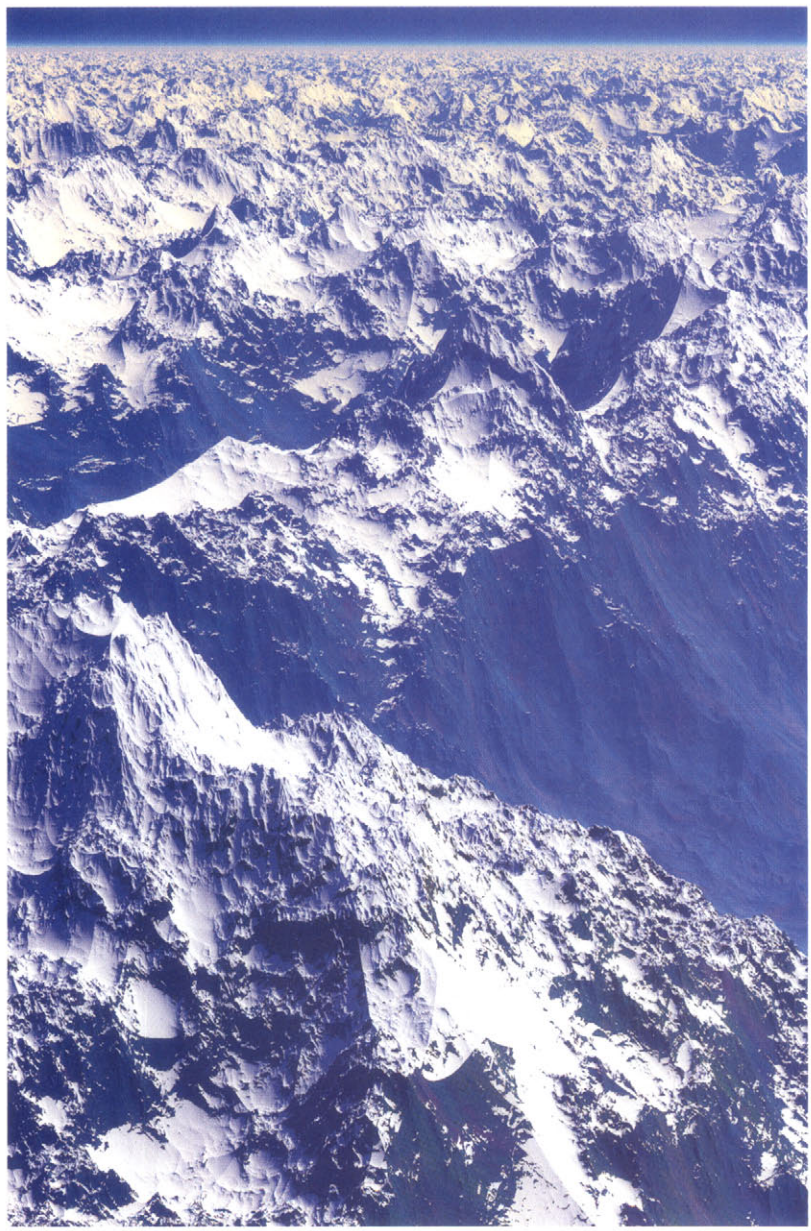

FIGURE 18.3 *Himalayas* shows color perspective over a long distance. Note that the white peaks turn red, while the dark areas turn blue with distance. Copyright © F. Kenton Musgrave.

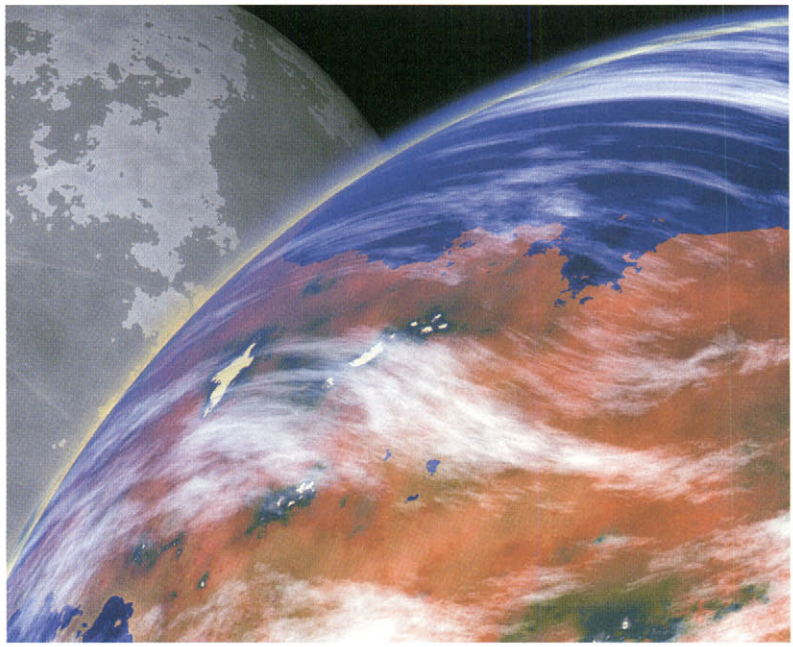

FIGURE 18.4 A detail of Figure 20.4 illustrates color perspective in a planetary atmosphere. This is the e^{-r^2} atmosphere model. Copyright © F. Kenton Musgrave.

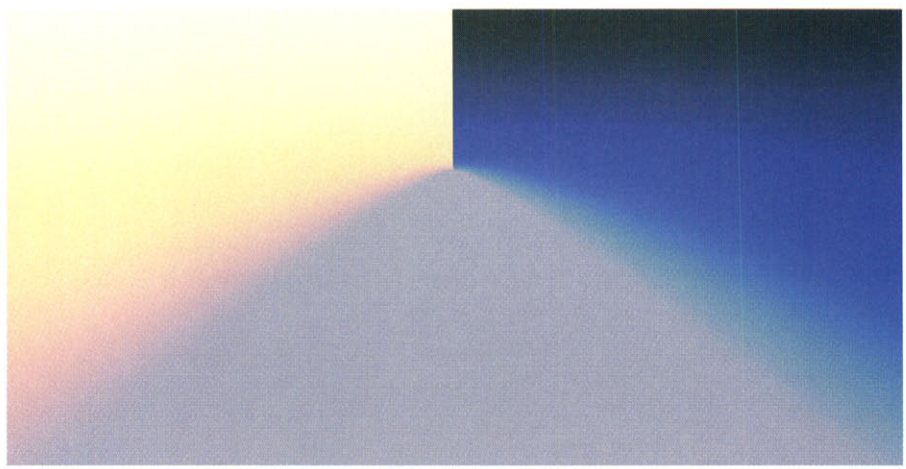

FIGURE 18.5 Color perspective in raw form. Two parallel vertical planes, one black and one white, illustrate how color changes with distance. The atmosphere is an exponential mist. Copyright © F. Kenton Musgrave.

To illustrate the simplicity of these two models, we now present pseudocode for the $\sigma = e^{-r^2}$ GADD with our Rayleigh scattering approximation:

```
/* compute distance from ray origin to closest approach */
adjacent_leg = ray.origin - fog.origin;
beta = DOT(ray.dir, adjacent_leg);
nearval = erf(sqrt(B) * beta);
farval = erf(sqrt(B) * (beta + t_e));
/* compute distance from fog origin to ray's closest approach */
r_c_squared = DOT(adjacent_leg,adjacent_leg) - beta*beta;
/* compute scattering approximation */
T = exp(-tau.red);
red = endpoint.red*T + (1.0-T)*atmosphere.red;
T = exp(-tau.green);
green = endpoint.green*T + (1.0-T)*atmosphere.green;
T = exp(-tau.blue);
blue = endpoint.blue*T + (1.0-T)*atmosphere.blue;
```

TRAPEZOIDAL QUADRATURE OF $\sigma = e^{-r}$ GADD AND RENDERMAN IMPLEMENTATION

For GADDs that are not integrable analytically, we must develop numerical quadrature (i.e., integration) schemes. The quadrature method may be arbitrarily sophisticated, according to the required accuracy. We now present an adaptive trapezoidal quadrature with sufficient accuracy for visual purposes and a RenderMan implementation of it.

Perhaps the most accurate, simple radial GADD is

$$\sigma(r) = Ae^{-Br}$$

where A modulates density at sea level, B is the falloff coefficient, and r is the height above sea level. For exponential GADDs, the density and its rate of change are greatest close to the planet surface. This indicates quadrature (integration) with an adaptive step size. Step size should be inversely proportional to the local magnitude of σ. Thus where the density and its rate of change in density are high, the step size is small; where the density is low, the step size is relatively large. To speed up rendering, we can employ a trivial reject if the ray never comes within a minimal distance to the GADD center, returning zero when we know the integral must be very small. Also, we can integrate separately forward and backward from the point of closest approach; this may increase accuracy through preventing overly large step sizes, by basing step size on the interval end of higher density. At each step we sample both the GADD and the illumination at the sample point.

Trapezoidal integration implies an assumption that the GADD varies linearly between the samples. The optical depth of a given interval is then

$$\tau = \frac{\Delta}{2}(\sigma_i + \sigma_{i-1})$$

where Δ is the step size, and σ_i and σ_{i-1} are the current and previous GADD density values. Differential extinction

$$dO = 1 - e^{-\tau}$$

and scattering

$$dC = I(1 - e^{-\tau})$$

where I is the direct illumination intensity at the sample point.

These differential values are then accumulated similarly to Drebin, Carpenter, and Hanrahan (1988). The RenderMan implementation operates in such a way that the atmosphere is shadowed where the light source is occluded by mountains, the planet, and so forth. If occluding features may be small, you must specify suitably low upper bounds on step sizes to prevent undersampling of shadow features.

Our implementation is as a volume shader in the RenderMan shading language (Upstill 1990). A simplified version of the shader follows. In Figure 18.6 a similarly structured light source shader causes the local illumination to undergo proper extinction. This and the full, more accurate volume shader are available on this book's Web site (*www.mkp.com/tm3*).

```
/* For ray index t, return the GADD (g) and illumination (li). */
#define GADD(li,g) \
      PP = origin + t * IN; \
      g = (density * exp(-falloff*(length(PP)-1))); \
      PW = transform ("shader", "current", PP); \
      li = 0; \
      illuminance (PW, point(0,0,1), PI) { li += Cl; }

volume radial_atmosphere (float density = 3.0, falloff = 200.0;
    float integstart = 0.0, integend = 10.0, rbound = 1.05;
    float minstepsize = 0.001, maxstepsize = 1.0, k = 35.0;)
{
    float t, tau, ss, dtau, last_dtau, te;
    color li, last_li, lighttau;
    point origin = transform("shader", P+I);
    point incident = vtransform("shader", -I);
    point IN = normalize(incident);
```

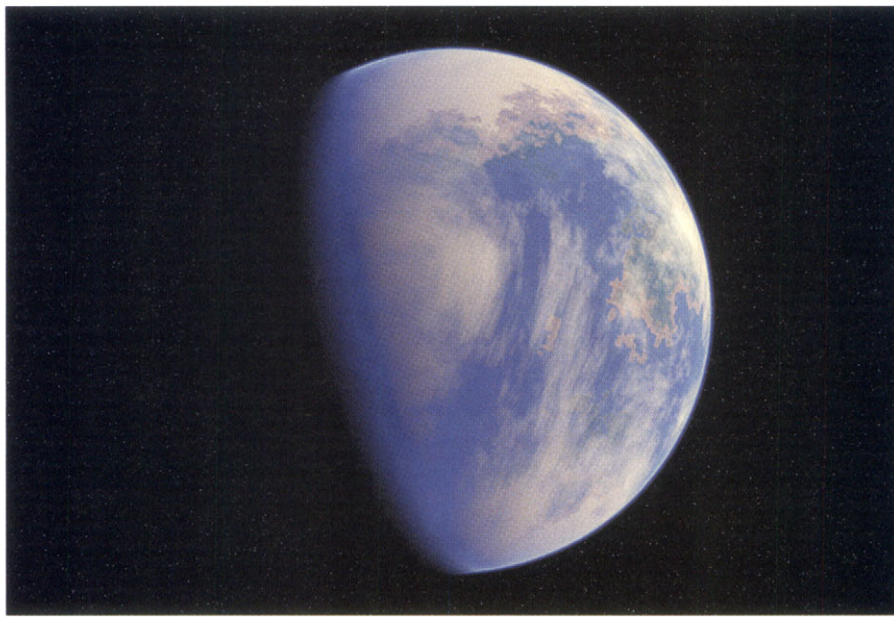

FIGURE 18.6 A raymarched e^{-r} planetary atmosphere model, implemented as a RenderMan shader. Such a model can yield more realistic coloring by including color extinction in the illumination. Copyright © F. Kenton Musgrave.

```
point PP, PW;
color Cv = 0.0, Ov = 0.0;  /* net color & opacity over optical path */
color dC, dO;              /* differential color & opacity */

/* compute optical path length */
te = min(length(incident), integend) - 0.0001;
/* integrate forward from the eye point */
t = integstart;
GADD(li, dtau)
ss = min(clamp(I/(k*dtau+0.001), minstepsize, maxstepsize), te-t);
t += ss;
while (t <= te) {
    last_dtau = dtau; last_li = li;
    GADD (11, dtau)
    /* compute dC and dO, the color and opacity of the portion
     * of the interval covered by this step */
    tau = 0.5 * ss * (dtau + last_dtau);
    lighttau = 0.5 * ss * (li*dtau + last_li*last_dtau);
    do = 1 - color (exp(-tau), exp(-tau*2.25), exp(-tau*21.0));
    dC = lighttau * dO;
```

```
        /* Adjust Cv and Ov to account for dC and dO */
        Cv += (1.0-Ov)*dC;
        Ov += (1.0-Ov)*dO;
        /* Select next step size and take a step */
        ss = min(clamp(I/(k*dtau+.001), instepsize, maxstepsize), te-t);
        ss = max(ss, 0.0005);
        t += ss;
    }

    /* Ci & Oi are the color and opacity of the background element.
     * Cv & Ov are the color and opacity of the atmosphere along the viewing ray.
     * Composite them together.
     */
    Ci = 15.0*Cv + (1.0-Ov)*Ci;
    Oi = Ov + (1.0-Ov)*Oi;
}
```

NUMERICAL QUADRATURE WITH BOUNDED ERROR FOR GENERAL RADIAL GADDS

The previous integration method for the e^{-r} GADD capitalizes on the smooth character of that GADD. As we may sometimes desire an error-bounded integration scheme suitable for more general radial GADDs, we now present such a scheme. As τ may be evaluated for every ray in a rendering, we require efficiency in its computation. Our knowledge of the integrand may be used to derive a suitable algorithm. Consider the general radial GADD $\sigma(r(t))$, where

$$r(t) = \sqrt{\alpha^2 + 2\beta t + t^2}$$

We can simplify by completing the square:

$$r(t) = \sqrt{(t - t_c)^2 + r_c^2}$$

where r_c is the value of r at the closest point on the line containing the ray to the center $\vec{o}$ of the radial GADD, and t corresponds to the t_c index at this closest approach. (This t_c might lie beyond the ray's extent on that line.) We can then make the substitution $s = t - t_c$ and rewrite the integral:

$$\tau = \int_0^{t_e} \sigma\left(\sqrt{\alpha^2 + 2\beta t + t^2}\right) dt = \int_{t_c}^{t_e - t_c} \sigma\left(\sqrt{s^2 + r_c^2}\right) ds$$

The integrand is symmetric about $s = 0$. If the limits of integration straddle 0, this symmetry can reduce the work of the numerical integrator by up to half. We can

also specify a bounding radius for the atmosphere, that is, where the integral of an infinite optical path ultimately maps to a luminance value of zero. Let us specify this radius as $r_{\max}$. Since

$$r = \sqrt{s^2 + r_c^2}$$

the bound is

$$s = \pm\sqrt{r_{\max}^2 + r_c^2}$$

We can also trivially set $\tau = 0$ if $r_c > r_{\max}$.

We are ultimately computing a transparency value that is in turn used to compute a quantized luminance sample. For 8-bit quantization, an error in e^{-r} of less than $\varepsilon = \pm\frac{1}{512}$ is insignificant. The symmetric integrand and high error tolerance allow for a specialized adaptive integration routine. An outline of a simple algorithm of this type follows; it returns a guaranteed bounded estimate for any radial GADD that decreases monotonically with radius.

1. Compute distance of closest approach r_c and ray index t_c at r_c.
2. If $r_c > r_{\max}$, return 0. Let radial cutoff bound

   $$s_m = \sqrt{r_{\max}^2 + r_c^2}$$

   If $s_m > t_c$, return 0. Compute integration bounds a and b: set $a = -\min(t_c, s_m)$. Set $b = -\min(t_e - t_c, s_m)$; if $b < -s_m$, return 0.
3. If $a < 0$ and $b > 0$, define two "regions" $R^{[1,2]}$. Region $R^{[1]}$ has left bound $R_l^{[1]} = 0$, right bound $R_r^{[1]} = \min(-a,b)$, and a weight R_w of 2.0; region $R^{[2]}$ has left and right bounds $R_l^{[2]} = \min(-a,b)$, $R_r^{[2]} = \max(-a,b)$, and a weight $R_w = 1.0$. Otherwise, make a single region with $R_l = a$ and $R_r = b$, with $R_w = 1.0$.
4. Compute the values of σ at left and right region bounds; label them $R_{\sigma l}$ and $R_{\sigma r}$. The maximum error $R_{\delta\tau}$ for the region, assuming Euler integration (i.e., the worst case), is $|R_{\sigma r} - R_{\sigma l}|(R_r - R_l)R_w$. The trapezoidal estimate for the region's integral R_τ is $\frac{1}{2}(R_{\sigma l} + R_{\sigma r})(R_r - R_l)$.
5. The total error

   $$\delta\tau = \sum_R R_{\delta\tau}$$

The total integral estimate

$$\tau = \sum_R R_\tau$$

If

$$\left(e^{\delta\tau-\tau} - e^{-\tau}\right) \leq \varepsilon$$

return τ.

6. Find the region with the highest error estimate. Bisect that region; one evaluation of σ is required. Compute integral and error estimates for both new regions. Go to step 5.

Potential modifications to this algorithm include splitting several regions at a time to allow less frequent checks of the error criterion and using Simpson's rule for integration.

CONCLUSION

We have presented a series of GADD models of increasing fidelity to the geometry of a planetary atmosphere. We have suggested a Rayleigh scattering model at a level of fidelity comparable to the ambient/diffuse/specular surface illumination model (i.e., highly nonphysical but simple, intuitive, and useful). We have illustrated the successful use of these models in image synthesis. Occam's Razor may recommend these models due to their simplicity; indeed, some are simple enough to be candidates for hardware implementation in real-time graphics systems. RenderMan implementations of these models are available on this book's Web site (*www.mkp.com/tm3*).